Predictive Thermal Control (PTC) Technology to enable Thermally Stable Telescopes: First Two Year Status

H. Philip Stahl and Thomas E. Brooks

NASA MARSHALL SPACE FLIGHT CENTER, HUNTSVILLE, AL 35812

ABSTRACT

The Predictive Thermal Control Technology (PTCT) development project is a multiyear effort initiated in Fiscal Year (FY) 2017, to mature the Technology Readiness Level (TRL) of critical technologies required to enable ultra-thermally-stable ultraviolet/optical/infrared (UVOIR) space telescope primary-mirror assemblies for ultra-high-contrast observations of exoplanets. Key accomplishments of 2017 to 2019 include: creating a high-fidelity STOP model of the AMTD-2 1.5-m Ultra-Low Expansion (ULE®) mirror (manufactured by Harris Corp) by merging 3D X-Ray computed tomography data of the 'as-built' mirror and coefficient of thermal expansion (CTE) data maps for each of the 18 core elements; partially validating this model by measuring the mirror's response to bulk temperature changes and lateral thermal gradients; designed and built (with PTC partner Harris Corp) a 1.5-m enclosure with 26 actively-control thermal zones; and defined specifications for a potential 4-m primary mirror thermal enclosure for the Habitable Exoplanet (HabEx) Imager mission

Keywords: thermal control, space telescopes, astrophysics, astronomy, HabEx

1. INTRODUCTION

"Are we alone in the Universe?" is probably the most compelling science question of our generation. Per the 2010 *New Worlds, New Horizons* Decadal Report[1]: "One of the fastest growing and most exciting fields in astrophysics is the study of planets beyond our solar system. The ultimate goal is to image rocky planets that lie in the habitable zone of nearby stars." The Survey recommended, as its highest priority, medium-scale activity such as a "New Worlds Technology Development (NWTD) Program" to "lay the technical and scientific foundations for a future space imaging and spectroscopy mission." The National Research Council (NRC) report, *NASA Space Technology Roadmaps & Priorities*[2], states that the second highest technical challenge for NASA regarding expanding our understanding of Earth and the universe in which we live is to "Develop a new generation of astronomical telescopes that enable discovery of habitable planets, facilitate advances in solar physics, and enable the study of faint structures around bright objects by developing high-contrast imaging and spectroscopic technologies to provide unprecedented sensitivity, field of view, and spectroscopy of faint objects." *NASA's Enduring Quests Daring Vision*[3] called for a surveyor mission to "enable ultra-high-contrast spectroscopic studies to directly measure oxygen, water vapor, and other molecules in the atmospheres of exoEarths," and "decode the galaxy assembly histories through detailed archeology of their present structure." As a result, NASA will study in detail a LUVOIR surveyor and a HabEx Imager concept for the 2020 Decadal Survey.[4,5] Additionally, AURA's *From Cosmic Birth to Living Earths*[6] details the potential revolutionary science that could be accomplished from "directly finding habitable planets showing signs of life."

Directly imaging and characterizing habitable planets requires a large-aperture telescope with extreme wavefront stability. For an internal coronagraph, this requires correcting wavefront errors (WFEs) and keeping that correction stable to a few picometers root mean square (rms) for the duration of the science observation. This places severe specification constraints on the performance of the observatory, telescope, and primary mirror. Per the 2015 Cosmic Origins Program Annual Technology Report (PATR)[7], a "Thermally Stable Telescope" is critical, highly desirable technology for a strategic mission. "*Wavefront stability is the most important technical capability that enables 10^{-10} contrast exoplanet science with an internal coronagraph. State of art for internal coronagraphy requires that the telescope must provide a wavefront that is stable at levels less than 10 pm for 10 minutes (stability period ranges from a few minutes to 10s of minutes depending on the brightness of the star being observed and the wavefront-sensing technology being used).*"

2. STATE OF THE ART

Thermal wavefront error occurs because of coefficient of thermal expansion (CTE); slewing the telescope relative to the sun causes its structure or mirrors to change temperature. Thermal heat load changes cause the structure holding the mirrors to expand/contract and the mirrors themselves to change shape. Fortunately, thermal drift tends to be slow, i.e. many minutes to hours. It is assumed that any drift that is longer than the WFSC control cycle will be corrected by a deformable mirror. Thus, we are only concerned about stability errors that are shorter than 10 to 120 minutes. State-of-the-art (SOA) for ambient temperature space telescopes are 'cold-biased' with heaters. The telescope is insulated from solar load such that, for all orientations relative to the sun, it is always at a 'cold' temperature (for example, 250K). The telescope is then warmed to an ambient temperature via heater panels on the forward straylight baffle tube as well as behind and beside the mirror.

No previous telescope has ever required picometer wavefront stability. Hubble Space Telescope (HST) and JWST illustrate the challenge. JWST is in the shadow of its sun-shade in a thermally stable SE-L2 orbit. HST is in a heated tube in a thermally varying low-Earth orbit. When JWST slews from its coldest to its warmest pointing, its temperature is predicted to change by 0.22K and its WFE is predicted to change by 31 nm rms. While not designed to do exoplanet science, it would take JWST over 14 days to 'passively' achieve the required level of stablity (Figure 1)[8]. Obviously, this is too long for exoplanet science. HST is a cold-biased telescope heated to an ambient temperature. But, this environment is not controlled. The HST telescope's temperature changes by nearly 20C as it orbits[9] – moving in and out of the Earth's shadow. This change causes the structure between the primary and secondary mirrors to change (typically ±3 µm) resulting in WFE changes of 10–25 nm every 90 min (Figure 2).[9] Assuming linear performance, HST could be used for exoplanet science if its thermal variation were controlled to <20mK.

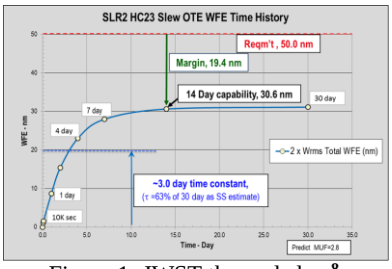

Figure 1: JWST thermal slew[8]

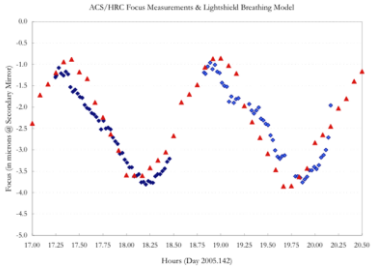

Figure 2: HST Orbit Focus[9]

When a telescope such as HST or JWST slews or rolls relative to the sun, the heat load on to the telescope's side and back changes - introducing axial and lateral gradients. These gradients cause the WFE to drift until the mirror reaches a new thermal equilibrium. The dominant WFE is power. The exact amplitude depends on the magnitude of the heat load change and the CTE of the mirror and structure.

To solve the focus problem, active thermal control was developed. For example, the commercial NextView telescope system manufacture by PTCT partner Harris Corporation has a 'bang/bang' thermal control system. Similar to a typical home thermostat, sensors are attached to the telescope's structure and if its temperature drops below a 'set point', the heaters turn on. Once the temperature reaches another set point, they turn off (Figure 3). The NextView thermal control system telescope's dead-band is ±300mK. The actual telescope temperature varies over a wider range (~±1K). While more than sufficient for commercial imaging, it is insufficient for exoplanet science. Current state-of-the-art thermal control uses proportional heater control (Figure 4). PTCT partner Harris Corp has demonstrated TRL-9 proportional thermal control on their Spaceview™ telescopes. Their thermal control system's sensors have a noise of ~50-mK and controls the 1.1-m telescope to a temperature of 100 to 200-mK.[10]

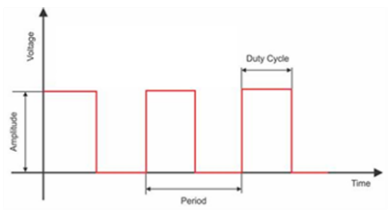

Figure 3: Bang/Bang Control Cycle

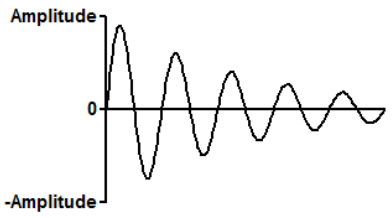

Figure 4: Proportional Control Cycle

3. PREDICTIVE THERMAL CONTROL

Our concept is to place the primary mirror inside a thermal enclosure that can 'sense when' and/or 'predict how' the telescope's external thermal load changes (because of a slew or roll relative to the sun) and modifies the amplitude of its zonal heaters to compensate, an approach called Predictive Thermal Control (PTC). PTC places a predictive thermal model in the control loop to intelligently control a system's thermal state. PTC uses sensors to measure the temperature distribution on the optic to estimate temperatures at unmeasured locations and determines the resulting heating profile needed to produce the desired temperature profile. Based on a given slew or roll, the Model knows how the thermal load will change, how it will propagate through the insulated outer barrel, and how it will affect the telescope. Sensors in the outer barrel will confirm these predictions. The control system increases or decreases heater output in the appropriate zone of the forward tube or mirror thermal enclosure to compensate. The telescope primary mirror should see no temperature change, regardless of where the telescope points on the sky.

PTCT plans to advance the SOTA in thermal control by comparing current SOTA to new logic like Model Predictive Control (MPC) or a narrow artificial intelligence (AI).[11,12] There are several potential MPC architectures, but an example MPC architecture places a physics-based model into the control loop to determine control variables (heater power levels) based on state variables (temperature measurements). MPC determines heater power levels using a completely different logic than proportional control. Proportional control adjusts heater power in proportion to the difference between measured and desired temperatures at a single location following an equation:

$$Q_i = K_p * (T_{d,i} - T_{m,i})$$

Where K_p is the proportional gain coefficient, $T_{d,i}$ is the desired temperature at control zone i, and $T_{m,i}$ is the measured temperature at control zone i. MPC uses multiple control zones. MPC starts with a system of equations based on the physics governing a control case. Then, to achieve control, uses a numerical version of the heat equation to back solve for the heat distribution that gives the desired temperature distribution:

$$\frac{2C_i}{\Delta t}\left(T_i^{n+1} - T_i^{n}\right) = 2Q_i + \sum_{j=1}^{N}\left[G_{ji}\left(T_j^{n} - T_i^{n}\right) + \hat{G}_{ji}\left\{\left(T_j^{n}\right)^4 - \left(T_i^{n}\right)^4\right\}\right] + \sum_{j=1}^{N}\left[G_{ji}\left(T_j^{n+1} - T_i^{n+1}\right) + \hat{G}_{ji}\left\{\left(T_j^{n+1}\right)^4 \left(T_i^{n+1}\right)^4\right\}\right]$$

MPC is superior to the proportional method because it takes into account the interdependency between all control zone's temperatures and all control zone's heater power. As an example, in a proportional system, if one control zone is too hot while a nearby control zone is too cold, the cold control zone's heater will turn on and exacerbate the already too hot control zone's problem. But, a MPC system will understand all interdependencies and command the heaters such that all zonal temperatures are considered and all zonal heaters work as a collective.

Finally, as shown in Figure 5, preliminary analysis[11, 12] indicates that (assuming that thermal performance is linear) it is possible to achieve pm wavefront stability by either controlling the shroud to a small temperature (10 mK) or by rapidly correcting the temperature. Additional stability can be achieved by increasing the system's thermal mass. This is particularly relevant to potential telescopes – such as HabEx – which might have large monolithic primary mirrors. Thus, as long as one senses faster than the mirror's thermal response time, there are a range of control solutions, and the faster the control cycle, the less precise the sensing needs to be.

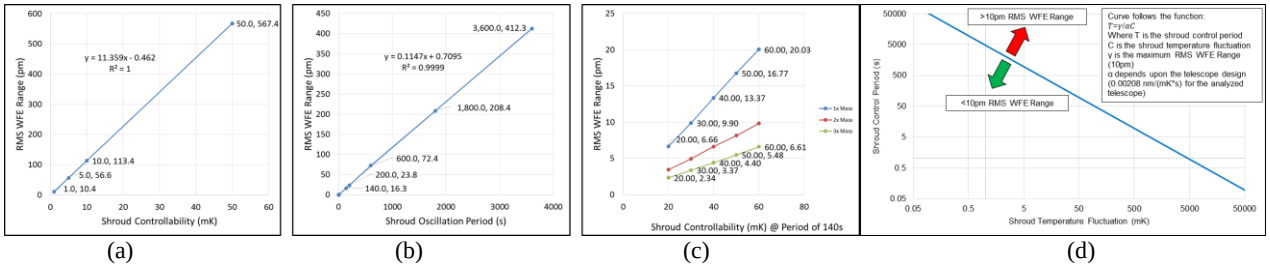

(a) (b) (c) (d)

Figure 5: (a) WFE versus shroud thermal control amplitude for 5,000 second control period. (b) WFE versus shroud control period for 50mK control amplitude. (c) WFE versus mirror mass and shroud control amplitude for 140 sec control period. (d) WFE stability tolerance can be achieved by a range of sensor noise uncertainty and control period.

4. GOALS AND OBJECTIVES

The 2015 PATR[7] assesses Thermally Stable Telescope technology to be Technology Readiness Level 3 (TRL-3). And, to advance this TRL:

> *"Significant technology development is needed to produce 'stable' isothermal or thermally 'insensitive' telescopes:*
> - *Thermal design techniques validated by traceable characterization testing of components;*
> - *Passive thermal isolation;*
> - *Active thermal sense at the < 0.1mK level; and*
> - *Active Thermal Control at the < 10 mK level.*
>
> *To move forward with confidence in designing such a thermal control system (for either monolithic or segmented mirror systems) requires validated thermal performance models. Technology development is required to produce validated models by making traceable components and sub-systems, using the models to make measurable performance predictions, and then quantifying these predictions by testing in a relevant environment."*

The goal of PTCT is to mature by at least 0.5 TRL step the technology needed for an exoplanet science thermally stable telescope by developing "thermal design techniques validated by traceable characterization testing of components". To achieve this goal, PTC has defined three objectives:

1. Validating models that predict thermal optical performance of real mirror assemblies based on their structural designs and constituent material properties, i.e., CTE distribution, thermal conductivity, thermal mass, etc.
2. Deriving thermal system stability specifications from wavefront stability requirement.
3. Demonstrating utility of a Predictive Control thermal system algorithm for achieving thermal stability.

To achieve these objectives, PTC has a detailed technical plan with five quantifiable milestones:

Milestone #1: Develop a high-fidelity model of the 1.5m ULE® AMTD-2 mirror.

Milestone #2: Derive specifications for thermal control system as a function of wavefront stability.

Milestone #3: Design and build a predictive Thermal Control System for a 1.5m ULE® mirror that senses temperature changes and actively controls the mirror's thermal environment.

Milestone #4: Validate high-fidelity model by testing the 1.5-m ULE® AMTD-2 mirror in a relevant thermal vacuum environment at the MSFC X-ray and Cryogenic Facility (XRCF) test facility.

Milestone #5: Use validated model to perform trade studies to optimize primary mirror thermo-optical performance as a function of mirror design, material selection, material properties (i.e., CTE) mass, etc.

Milestones #1 and #4 support Goal #1. Milestone #1 creates the high-fidelity model and Milestone #4 validates the model. Milestones #2 and #5 support Goal #2. And, Milestone #3 supports Goal #3.

The connection between Milestones and Goals may be slightly confusing, the Milestones were defined to be in a temporal sequential order. And, while Milestone #5 was not scheduled for completion until the end of PTC, because of the need to provide performance feedback to Milestone #2 and the needs of the HabEx mission concept study, Milestones #2 and #5 were performed in parallel.

5. PROGRESS AND ACCOMPLISHMENTS

5.1 Objective #1: Validated High-Fidelity Structural-Thermal-Optical-Performance (STOP) Model

Designing a telescope to have an ultra-stable wavefront requires using a validated high-fidelity STOP model to predict thermal optical performance of mirrors and structure based on their mechanical designs and material properties, i.e., CTE distribution, thermal conductivity, thermal mass, etc.

5.1.1 Milestone #1: Develop a high-fidelity STOP model of the1.5m ULE® AMTD-2 mirror.

A high-fidelity STOP model of the AMTD-2 1.5-m ULE® mirror was created in NASTRAN that accurately models its 'as-built' mechanical dimensions and 3D CTE distribution.[13] The 'as-built' mechanical dimensions were quantified using 3D X-ray computed tomography to measure the internal structure of the mirror and ported into a mechanical model (Figure 6). A custom algorithm was written to convert the X-ray CT 3D mapping into a finite element model. To add a 3D mapping of CTE distribution, Harris Corporation provided MSFC with Corning CTE data maps for each of the 18 core elements and the location of each element in the core (Figure 7).

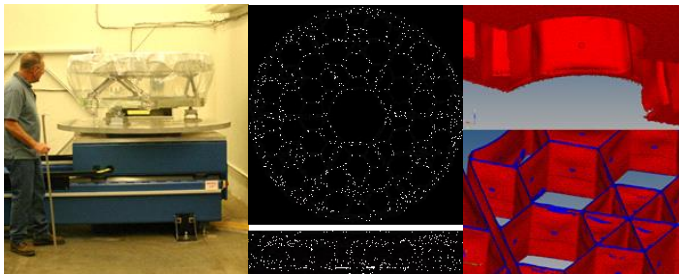

Figure 6: Internal dimensional structure of the 1.5-m AMTD-2 mirror was quantified via x-ray computed tomography and code was developed by MSFC to convert CT scan data into a finite element model.

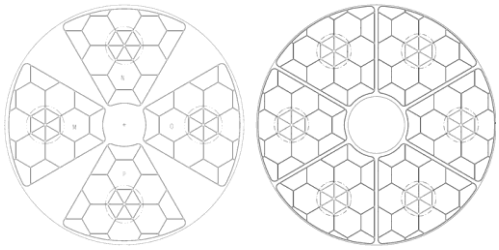

Figure 7: Harris Corp provided Corning CTE data of where each core element was cut from its boule (left) and the location of that core element in the AMTD-2 mirror (right).

5.1.2 Milestone #4: Validate high-fidelity STOP model by testing the 1.5-m ULE® AMTD-2 mirror in a relevant thermal vacuum environment at the MSFC X-ray and Cryogenic Facility (XRCF) test facility.

To validate the high-fidelity model, the 1.5-m ULE® AMTD-2 mirror's response to static thermal loads and lateral thermal gradients was tested in the XRCF. This test was conducted as part of the final AMTD-2 static thermal soak test. For model validation, the mirror was fully instrumented with sensors to provide knowledge of its temperature distribution during test (Figure 8).

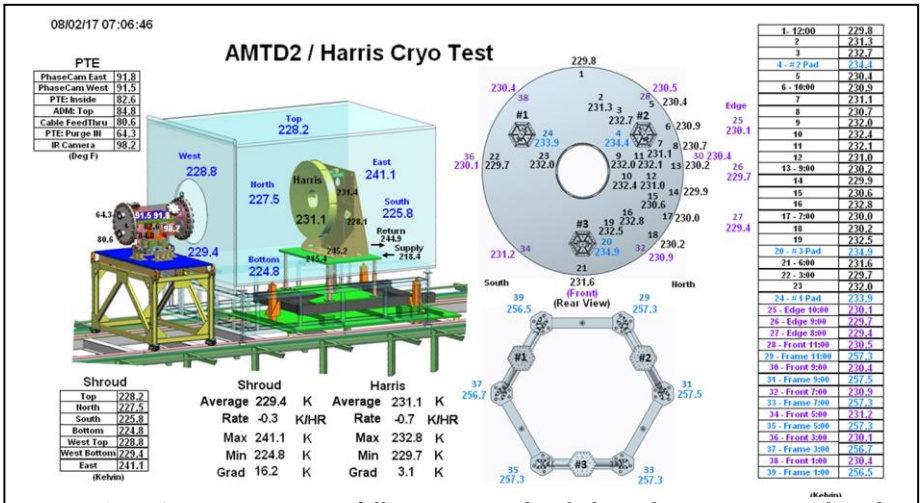

Figure 8: PTC test setup. Mirror fully instrumented with thermal sensors in cryo-shroud.

First, the high-fidelity model was correlated to the cryo-deformation of the AMTD-2 mirror measured during the static thermal load test. This deformation consists of two components: the opto-mechanical-thermal deformation of the mirror mount system and the mirror substrate's CTE distribution. As the temperature of the mirror and mount changes from 293 to 231K, the aluminum backplane contracts, and the mount struts apply a prying force to the mirror. The prying signature is not symmetric even though the design is symmetric, which means that the as-built mount has unintended asymmetries. The model applies prying forces directly to the bond pad and the combination of forces that most closely matches the test data was used to represent the effect of the bond pads. Based on the mirror's measured temperature deformation, the model predicts a mount distortion of 18.9-nm rms (Figure 9 left). CTE inhomogeneity also produce cryo-deformation. Figure 9 right shows a 16.6-nm rms surface shape that best fits the test data produced entirely by the mirror's 3D CTE distribution.

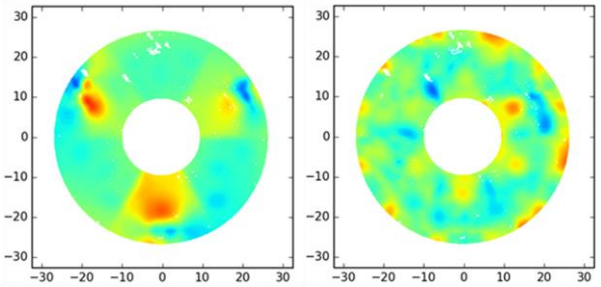

Figure 9: (left) Predicted 18.9 nm rms mount cryo-deformation. (right) Predicted 16.6 nm rms CTE cryo-deformation.

Combining mount and CTE effects, the high-fidelity model of the 1.5-m AMTD-2 ULE® mirror predicts 24.7-nm rms of the measured 28.8-nm rms leaving a 13.4-nm rms residual error (Figure 10).[14, 15]

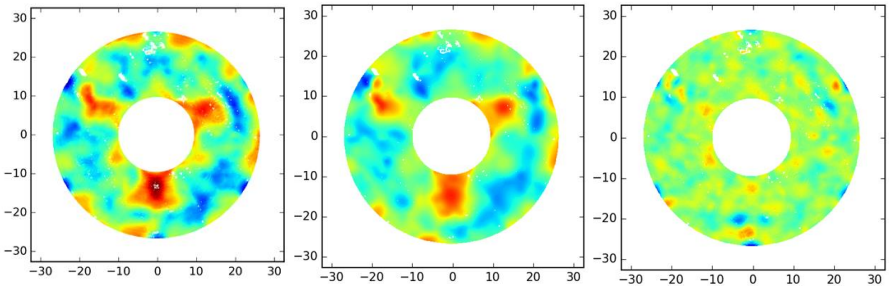

Figure 10. Left: Thermal soak of the mirror and mount going from 293 to 231 K had a measured cryo-deformation of 28.8-nm rms. Center: Model predicted 24.7-nm rms from mount effects and CTE inhomogeneity. Right: Residual error is 13.4-nm rms.[14, 15]

To further validate the high-fidelity model, the 1.5-m ULE® AMTD-2 mirror's response to a lateral thermal gradient was tested in the XRCF. PTC modified MSFC's XRCF facility to introduce thermal gradients into mirror systems using solar lamps (Figure 11). This test was a bare-mirror-only test, i.e. mirror only with no thermal control system – which will be done via Milestone #3. The solar lamps introduced a thermal gradient of 87.7 K into the mirror causing a 78.7-nm rms surface deformation (Figure 12).[16] The high-fidelity model was able to match this deformation by increasing the average CTE of the mirror substrate in the model to 81 ppb/K. As show in Figure 12d, Corning published data shows that ULE® bulk CTE changes from ~0 ppb/K at 20 C to approximately 70 to 80 ppb/K at 100C.[17]

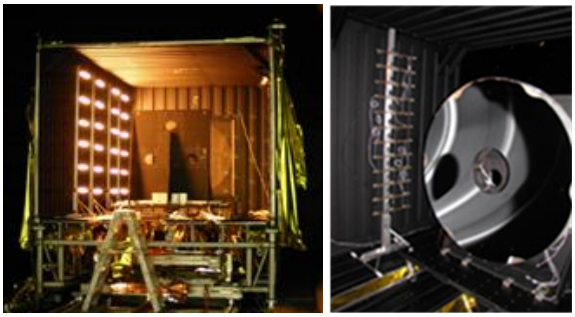

Figure 11: (left) Solar Lamp Array inside XRCF Cryo-shroud. (right) 1.5-m AMTD-2 ULE® mirror was tested with a single lamp array to impose lateral thermal gradient.

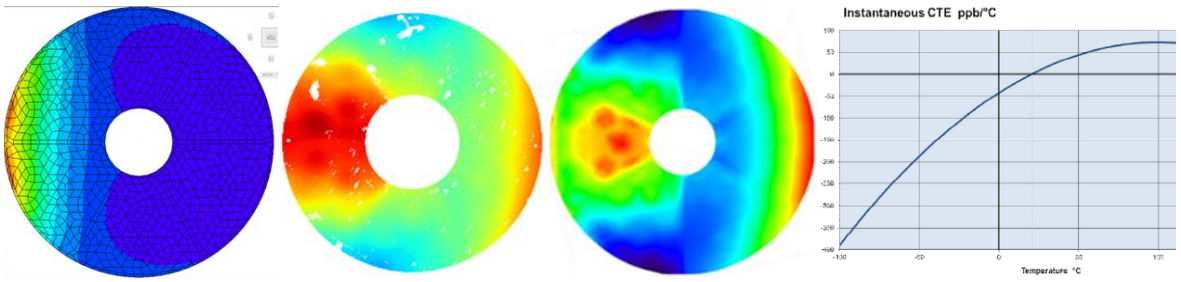

(a) *(b)* *(c)* *(d)*

Figure 12. (a) Temperature distribution (ΔT = 87.7K PV) calculated by Thermal Desktop from thermocouple data on mirror back for heat lamps outputting 406W. (b) Measured surface figure error (RMS = 78.5nm). (c) To match measured SFE caused by temperature distribution, model had to increase average substrate CTE to 81ppb/K.[16] (d) Per Corning, ULE® bulk CTE increases from ~0 ppb/K at 20C to ~70 to 80 ppb/K at 100C.[17]

5.2 Objective #2: Derive Traceable Specifications for an Active Thermal Control System

Designing a telescope to have an ultra-stable wavefront via active thermal control requires a validated STOP model to help define the thermal control system's performance specifications, such as: sensing resolution (1 or 10 or 50 mK), control accuracy (10 or 50 mK), control period (1 or 5 or 20 min), number and distribution of sense and control zones.

5.2.1 Milestone #2: Derive specifications for thermal control system as a function of wavefront stability.

Milestone #2 was completed by designing an active thermal control enclosure that achieves a HabEx engineering study team provided wavefront stability error budget for the baseline HabEx 4-m Zerodur® primary mirror design when exposed to a representative design reference mission. The specification was developed by deriving an error budget based on the vector vortex coronagraph's contrast leakage sensitivity to wavefront error decomposed into Zernike polynomials[18] and the measured thermal wavefront error performance of the Schott 1.2-m Zerodur® mirror characterized by the AMTD-2 project.[19] The resulting specification is for an active thermal control system with 86-control zones on the primary mirror and its hexapods, thermal sensors with 50-mK measurement uncertainty, and proportional controller systems (PID) operating with 30 second periods.

5.2.2 Milestone #5: Use validated model to perform trade studies to optimize primary mirror thermo-optical performance as a function of mirror design, material selection, material properties (i.e., CTE) mass, etc.

While Milestone #5 was not scheduled for completion until the end of PTC, the PTC program in conjunction with the HabEx study performed trade studies in FY18/19 that defined a baseline primary mirror design that optimizes predicted thermo-optical performance as a function of mirror design.[20, 21] Given the feedback loop between the primary mirror design and the thermal enclosure specifications, Milestone #5 and Milestone #2 had to be completed together.

5.2.3 Baseline HabEx Primary Mirror Active Control System

Deriving a specification for a potential HabEx primary mirror active control system required three steps. First was defining an error budget. Second was defining the baseline primary mirror's thermal sensitivity by creating a thermal model of the telescope. And third was exercising the thermal model for multiple (including one final) design reference missions (DRMs).

A Zernike polynomial based wavefront stability error budget was derived from the total maximum allowed vector vortex coronagraph leakage to detect an exoEarth.[18] The process starts by calculating the amount of raw contrast leakage that a coronagraph can have and still detect an exoplanet relative to its host star, at a defined signal to noise ratio. For the case illustrated in Figure 13, this is 40 parts-per-trillion. Next the contrast leakage sensitivity of the coronagraph is calculated for each Zernike polynomial. Finally, the allowed contrast leakage is allocated between Zernike polynomials and converted into wavefront error. For example, the vector vortex charge 4 coronagraph is insensitive to tilt and power, therefore, more error can be allocated to these terms. But, all higher order terms must be very stable. As shown in Figure 14, the error budget can be further sub-allocated between thermal, inertial and LOS WFE.

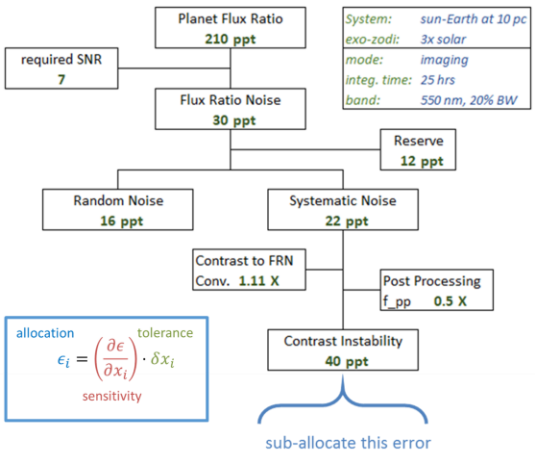

Figure 13: Wavefront Stability Error Budget Development Method.[18]

			Allocation	100%	30%	30%	30%	10%
Order				VVC-4 Tolerance	LOS	Inertial	Thermal	Reserve
K	N	M	Aberration	[pm rms]	[pm rms]	[pm rms]	[pm rms]	[pm rms]
			TOTAL RMS	1628.4	892	892	892	515
1	1	1	Tilt	1192.8	653.32	653.32	653.32	377.19
2	2	0	Power (Defocus)	1108.6	607.19	607.19	607.19	350.56
3	2	2	Pri Astigmatism	3.8	2.09	2.09	2.09	1.21
4	3	1	Pri Coma	3.3	1.81	1.81	1.81	1.05
5	3	3	Pri Trefoil	3.3	1.81	1.81	1.81	1.05
6	4	0	Pri Spherical	3.1	1.69	1.69	1.69	0.97
7	4	2	Sec Astigmatism	3.1	1.69	1.69	1.69	0.97
8	4	4	Pri Tetrafoil	3.0	1.62	1.62	1.62	0.94
9	5	1	Sec Coma	2.7	1.48	1.48	1.48	0.85
10	5	3	Sec Trefoil	2.7	1.48	1.48	1.48	0.85
11	5	5	Pri Pentafoil	2.7	1.48	1.48	1.48	0.85
12	6	0	Sec Spherical	2.7	1.48	1.48	1.48	0.85
13	6	2	Ter Astigmatism	2.1	1.13	1.13	1.13	0.65
14	6	4	Sec Tetrafoil	2.5	1.37	1.37	1.37	0.79
15	6	6	Pri Hexafoil	2.5	1.37	1.37	1.37	0.79
16	7	1	Ter Coma	1.4	0.77	0.77	0.77	0.45
17	7	3	Ter Trefoil	1.6	0.90	0.90	0.90	0.52
18	7	5	Sec Pentafoil	1.6	0.87	0.87	0.87	0.50
19	7	7	Pri Septafoil	1.8	0.98	0.98	0.98	0.56
20	8	0	Ter Spherical	0.7	0.37	0.37	0.37	0.22
21	8	2	Qua Astigmatism	1.0	0.55	0.55	0.55	0.32
22	8	4	Ter Tetrafoil	1.2	0.67	0.67	0.67	0.38
23	8	6	Sec Hexafoil	1.4	0.79	0.79	0.79	0.45
24	8	8	Pri Octafoil	1.4	0.75	0.75	0.75	0.43
25	9	1	Qua Coma	0.9	0.50	0.50	0.50	0.29
26	10	0	Qua Spherical	1.1	0.63	0.63	0.63	0.36
27	12	0	Qin Spherical	2.0	1.07	1.07	1.07	0.62

Figure 14: Allocation of WFE Stability between LOS, Inertial and Thermal Sources.

Next, an integrated observatory thermal model was created in Thermal Desktop using a geometry created in Pro-Engineer CAD. The Thermal Desktop model has 20K elements and calculates telescope's structure and mirror temperature distribution at 10K nodes. The temperature distribution for each node is mapped onto the NASTRAN FEM and the deflections created by each node's coefficient of expansion (CTE) is calculated using NASTRAN Solution 101. Rigid body motions (RBM) and mirror surface deformations are calculated from the NASTRAN deflections using SigFit. The primary and secondary mirror's mesh grids were sized to enable SigFit to fit thermally induced surface figure error (SFE) to higher order Zernike polynomials.

The model assumes multi-layer insulation (MLI) to control heat loss and to isolate thermal disturbances (i.e. the Sun). Radiators pull heat from the science instruments and spacecraft electronics. Because of the MLI and radiators, the payload is passively cold-biased and active thermal control is required to maintain the primary mirror at an operating temperature of ~270K. Without heaters, the model predicts a primary mirror temperature of 206K. The model assumes TRL-9 capabilities for the primary mirror thermal enclosure: sensors with 50-mK measurement uncertainty; and proportional controller systems (PID) operating with 30 second periods. The model has 86 control zones on the primary mirror and its hexapods. The model predicts that the primary mirror front surface will have ~200 mK 'trefoil' thermal gradient (Figure 15). The source of this gradient is thermal conduction into the hexapod struts. And, the model predicts that the mirror will have ~3 K front to back gradient.

The primary and secondary mirror coefficient of thermal expansion (CTE) are modeled as consisting of a uniform 'bulk' CTE and a CTE homogeneity distribution. The uniform CTE value determines the mirror's low-order shape response to bulk temperature changes, and/or gradient temperature changes (i.e. axial, radial or lateral). Such temperature changes can produce low-order errors such as power and astigmatism. The homogeneity distribution determines the mirror's mid-spatial response. The model calculates mirror shape changes from two effects: (1) response of mirror with uniform CTE to changes in temperature at each of the 10K nodes; and (2) response of a mirror with a CTE inhomogeneity distribution to a uniform bulk temperature change. One method to estimate CTE inhomogeneity is to measure the thermal deformation of the mirror and assume that CTE is linear with temperature. As part of the Advanced Mirror Technology Development (AMTD) project, a 1.2-m ELZM was measured to have an ~11 nm rms deformation over a 62K thermal range (from 292K to 230K). Figure 16 shows the measured error and its decomposition into Zernike polynomials.[19] The model assumes this measured thermal signature for its CTE inhomogeneity distribution.

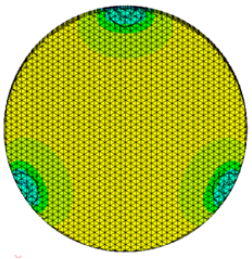

Figure 15: Predicted 200 mK trefoil thermal distribution of primary mirror front surface.

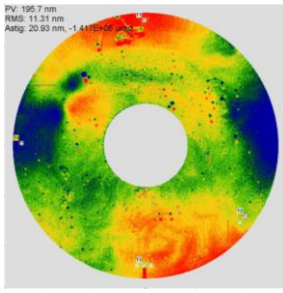

	Measured Delta-SFE 292-230K		
	Zernike Coefficient [nm] RMS Surface		
	RMS-Zern	X-Zern	Y-Zern
	[nm rms]	[nm rms]	[nm rms]
Aberration			
TOTAL RMS	26.016	nm rms	
Tilt	0.095	0.055	0.077
Power (Defocus)	0.416	0.416	
Pri Astigmatism	20.940	-19.960	-6.330
Pri Coma	2.541	-2.539	0.109
Pri Trefoil	6.089	-3.970	-4.617
Pri Spherical	0.599	0.599	
Sec Astigmatism	2.283	-2.046	-1.012
Pri Tetrafoil	5.471	-3.683	4.046
Sec Coma	2.591	-1.050	2.369
Sec Trefoil	4.811	0.912	-4.724
Pri Pentafoil	1.838	1.713	-0.666
Sec Spherical	1.067	1.067	
Ter Astigmatism	3.465	3.341	-0.918
Sec Tetrafoil	1.089	-0.647	0.876
Pri Hexafoil	4.772	-4.569	-1.376
Ter Coma	3.073	0.786	-2.971
Ter Trefoil	6.863	-1.165	6.763
Sec Pentafoil	1.953	-0.487	1.891
Ter Spherical	0.729	-0.729	
Qua Astigmatism	0.171	-0.091	-0.144
Ter Tetrafoil	1.999	1.262	-1.550
Qua Coma	3.659	3.220	-1.738
Qua Spherical	1.883	-1.883	
Qin Spherical	2.635	2.635	

Figure 16: 1.2m Schott ELZM 62K thermal deformation decomposed into Zernikes

The model was used to predict thermal performance for a potential science design reference mission (DRM). The DRM starts by pointing the telescope pointing at a reference star to dig the dark hole in the coronagraph. The analysis assumes that the telescope reaches a steady state thermal condition at this sun orientation. Next, the telescope is pointed at the science star. To make the analysis 'worst-case' it is assumed that when the telescope is pointing at the reference star, the sun is perpendicular to the sun-shade/solar-panels with a +θ degree roll. And, when it points at the science star, it pitches away from the sun (Figure 17). Figure 18 shows the DRM motions as viewed from the sun.

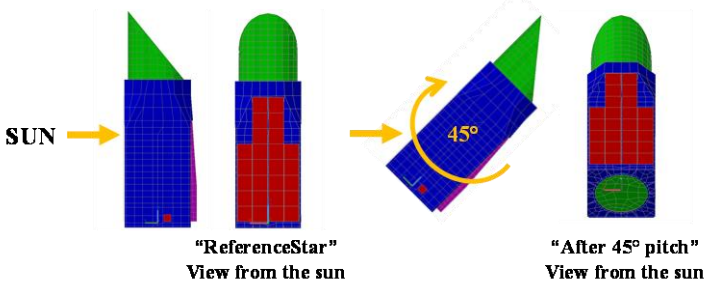

Figure 17: Nominal observing scenario slews for thermal analysis

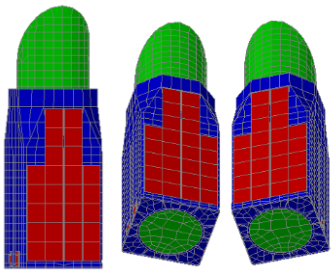

Figure 18: Telescope motions as viewed from the Sun

Figures 19 to 21 show how well the modeled active zonal thermal enclosure controls the temperature of the primary mirror for a DRM consisting a 75 degree pitch of the telescope after it has spent 20 hours pointing at a reference star to dig the dark hole followed by a 30 degree roll (from +15 deg to -15 deg) at 45 hours. Figure 19 shows the predicted change in average bulk temperature and axial gradient temperature of the primary mirror if there were no active control. Please note that the axial gradient changes faster than the average temperature, this will have WFE impact. Figures 20 and 21 show the predicted average and gradient temperature changes for the primary mirror under active thermal control. The zonal control system keeps the PM average bulk temperature change to less than ~0.035-mK and the axial gradient change to less than ~1.75-mK.

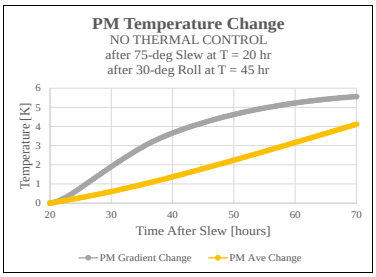

Figure 19: Passive PM average and axial gradient temperature change from 75 deg pitch.

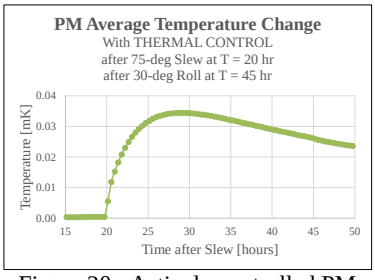

Figure 20: Actively controlled PM average bulk temperature change from 75 deg pitch.

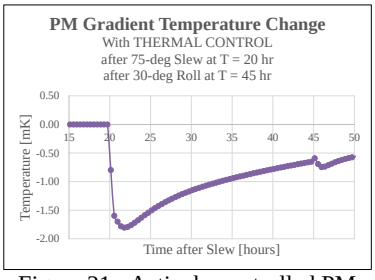

Figure 21: Actively controlled PM axial temperature gradient change from 75 deg pitch.

To calculate primary mirror wavefront stability, Thermal Desktop calculated its temperature distribution as a function of time and NASTRAN calculated the surface deformations produced by that distribution. The temporal WFE was then decomposed into Zernike polynomials by SigFit. Figure 22 shows the change in primary mirror WFE produced by the 75 degree thermal slew DRM with no active thermal control. Figure 23 shows the change in the primary mirror WFE caused by the 75-deg slew DRM with active zonal thermal control. Because the control system is able to keep the average and axial gradient temperatures very small, the Thermal WFE remains less than 1 picometer rms. As shown in Figure 24, the predicted primary mirror thermal WFE stability has significant performance margin relative to the error budget tolerance. The most important errors are astigmatism and coma.

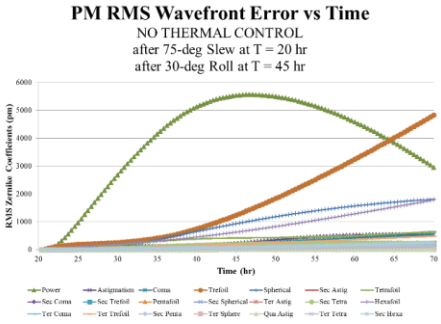

Figure 22: Changing PM Zernike WFE after 75-deg thermal slew with no thermal control

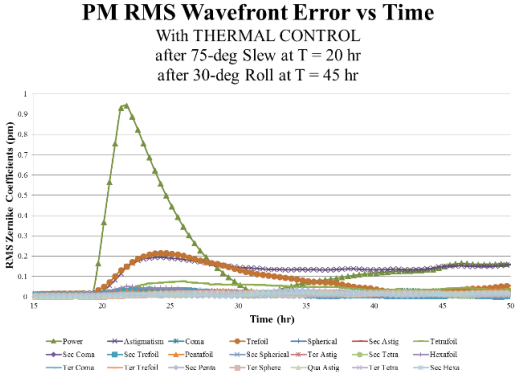

Figure 23: Changing PM Zernike WFE after 75-deg thermal slew with Active Zonal Thermal Control.

Order				Allocation Thermal	PM Allocation 50%	MARGIN	Zernikes Thermal WFE
K	N	M	Aberration	[pm rms]	[pm rms]		[pm rms]
			TOTAL RMS	814.22	575.74		1.990
1	1	1	Tilt	596.40	421.72	33469.48	0.013
2	2	0	Power (Defocus)	554.29	391.94	208.13	1.883
3	2	2	Pri Astigmatism	1.91	1.35	3.47	0.389
4	3	1	Pri Coma	1.65	1.17	15.90	0.074
5	3	3	Pri Trefoil	1.65	1.17	2.72	0.430
6	4	0	Pri Spherical	1.54	1.09	17.62	0.062
7	4	2	Sec Astigmatism	1.54	1.09	20.64	0.053
8	4	4	Pri Tetrafoil	1.48	1.05	6.86	0.153
9	5	1	Sec Coma	1.35	0.96	20.24	0.047
10	5	3	Sec Trefoil	1.35	0.96	14.05	0.068
11	5	5	Pri Pentafoil	1.35	0.96	14.17	0.067
12	6	0	Sec Spherical	1.35	0.95	37.30	0.026
13	6	2	Ter Astigmatism	1.03	0.73	13.99	0.052
14	6	4	Sec Tetrafoil	1.25	0.89	17.87	0.050
15	6	6	Pri Hexafoil	1.25	0.88	8.76	0.101
16	7	1	Ter Coma	0.70	0.50	10.09	0.049
17	7	3	Ter Trefoil	0.82	0.58	13.51	0.043
18	7	5	Sec Pentafoil	0.80	0.56	8.40	0.067
19	7	7	Pri Septafoil	0.89	0.63		0.000
20	8	0	Ter Spherical	0.34	0.24	5.81	0.042
21	8	2	Qua Astigmatism	0.50	0.36	8.78	0.041
22	8	4	Ter Tetrafoil	0.61	0.43	14.83	0.029
23	8	6	Sec Hexafoil	0.72	0.51	10.98	0.046
24	8	8	Pri Octafoil	0.68	0.48		0.000
25	9	1	Qua Coma	0.46	0.32		0.000
26	10	0	Qua Spherical	0.57	0.40		0.000
27	12	0	Qin Spherical	0.98	0.69		0.000

Figure 24: PM Thermal WFE meets its tolerance.

5.3 Objective #3: Demonstrate utility of Predictive Control thermal system for achieving thermal stability.

Building a telescope that has an ultra-stable wavefront requires an active thermal control system that is beyond the current state of art (i.e., bang-band or proportional control). The goal of Objective #3 is to demonstrate the ability of advanced control algorithms to control a mirror's shape by determining control variables (heater power levels) based upon state variables (temperature measurements).

5.3.1 Milestone #3: Design, build, and test a predictive thermal control system

PTCT Partner, Harris Corp designed and built a thermal enclosure with 37 control zones for the 1.5-m AMTD-2 mirror. It has been delivered to MSFC (Figure 25) and is being integrated with the PTC control electronics and software.

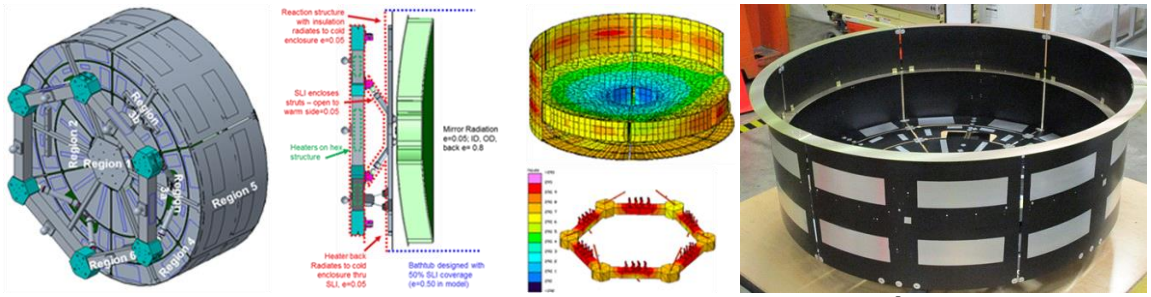

Figure 25: Thermal Control System with 37 zone control for AMTD-2 1.5-m ULE© mirror (ITAR)

PTC will be considered demonstrated if it can correct for externally imposed thermal gradients (i.e., radial, lateral, and axial gradients). Other goals include: self-tuning thermal parameters in the thermal model to improve the PTC's

veracity, informing the design of enclosure hardware and thermal shrouds to enable controllability, and directly imposing measurable thermally-induced WFE into the mirror (Figure 26).

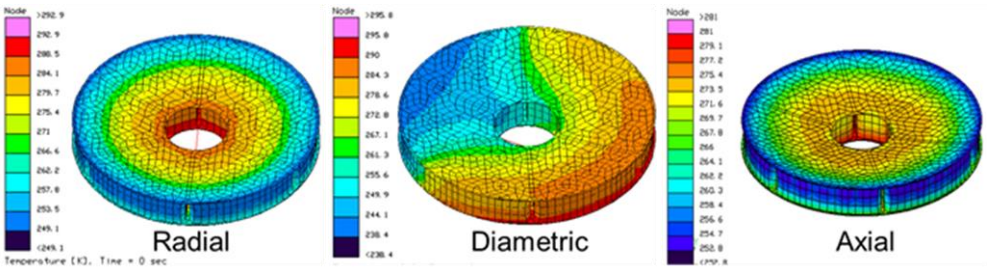

Figure 26: Thermal Control System can introduce Radial, Lateral and Axial thermal gradients.

Because when we perform the Milestone #3 tests, the thermal enclosure will prevent direct illumination of the mirror from the solar lamps, STOP analysis predicts that the 1.5-m ULE® mirror – when integrated with the enclosure – will experience only a 7.5 nm rms figure change without thermal control; and, with thermal control this change is reduced to 1.5 nm rms (Figure 27). For this reason PTC decided to procure a 1.2-m aluminum mirror to serve as a pathfinder test article (Figure 28). Since aluminum has a larger CTE than ULE®, it is expected to provide a 2X larger signature – which can be used to practice the PTC control algorithm.

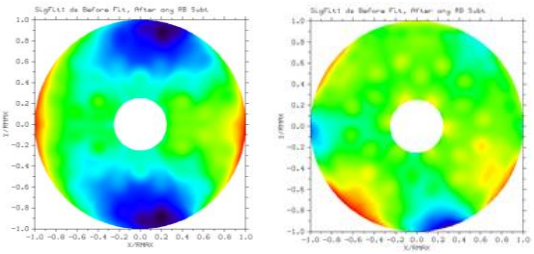
Figure 27: (left) Predicted SFE without thermal control. (right) Predicted SFE with thermal control correction.


Figure 28: 1.2-m Al Test Mirror

Additionally, in support of a potential Origins Space Telescope (OST) mission, PTC obtained MSFC IRAD funds to test the aluminum mirror at 30K to characterize its cryo-deformation for a cryo-null polishing demonstration. And, to cycle this mirror to 30K three times to quantify any cryo-creep effects.

6. CONCLUSION

The Predictive Thermal Control Technology (PTCT) project is a multi-year effort to mature TRL of technologies needed to enable ultra-thermally-stable ultraviolet/optical/infrared (UVOIR) space telescope primary-mirror assemblies for ultra-high-contrast observations of exoplanets. Recent accomplishments include: using X-ray computed tomography to create a high-fidelity STOP model of the AMTD-2 1.5-m Ultra-Low Expansion (ULE®) mirror (manufactured by Harris Corp); validating that model by test in an updated MSFC XRCF; building (with PTC partner Harris Corp) a 1.5-m enclosure with 26 actively-control thermal zones; and defined specifications for a potential 4-m primary mirror thermal enclosure for the Habitable Exoplanet (HabEx) Imager mission.

ACKNOWLEDGEMENTS

PTC is a funded by a NASA Science Mission Directorate (SMD) Astrophysics Division (APD) Directed Work Package.

Others contributing to the work summarized in this paper include (in alphabetical order) from NASA MSFC: Pat Bagley, Mark Baker, Ron Beshears, Michael R. Effinger, Ron Eng, Randy Goode, Charlie Griffith, Harlan Haight, Thomas Hill, Bill Hogue, Steve Johnson, Jeff Kegley, Darron Rice, Harry Rutledge, Richard Siler, W. Scott Smith, Ernie Wright and Roy Young; ESSCA: Jim Duffy, Art Lapietra, Terry Lee, Scott Marona, Zakkary McPeters, John Tucker, and Mark Young; AI Systems: William Arnold; NASA Pathways Interns: Meghan Carrico, Adam Cedrone and Tim Little; and from Harris Corp: Jesse Cramer, Robert Day, Robert Egerman, Scott Gade, Keith Havey, Carl Rosati, and Piero Terio

REFERENCES

1. Committee for a Decadal Survey of Astronomy and Astrophysics; National Research Council, New Worlds, New Horizons in Astronomy and Astrophysics, The National Academies Press, Washington, D.C., 2010.
2. NASA Space Technology Roadmaps and Priorities: Restoring NASA's Technological Edge and Paving the Way for a New Era in Space, NRC Report, 2012.
3. Kouveliotou, Centrella, Peterson, et al, Enduring Quests, Daring Visions: NASA Astrophysics in the Next Three Decades, 2014, arXiv:1401.3741, 2014.
4. Hertz, Paul, "Planning for the 2020 Decadal Survey: An Astrophysics Division White Paper", January 4, 2015, available at science.nasa.gov/astrophysics/documents/.
5. NASA Town Hall, AAS Winter Meeting, Kissimmee, FL, 2016.
6. Dalcanton, Seager, et al, From Cosmic Birth to Living Earths: The Future of UVOIR Space Astronomy, Association of Universities for Research in Astronomy, 2015, www.hdstvision.org/report/.
7. "Cosmic Origins Program Annual Technology Report", 2015.
8. 13-JWST-0207 F, 2013.
9. Lallo, Matthew D., Experience with the Hubble Space Telescope: 20 years of an archetype, 2012, Opt. Eng. Vol. 51, 011011, January 2012, doi: 10.1117/1.OE.51.1.011011.
10. Havey, Keith, Harris Corporation, Private Communication, 13 March 2019.
11. Brooks, Thomas, H. Philip Stahl, William R. Arnold, "Advanced Mirror Technology Development (AMTD) thermal trade studies", Proc. SPIE 9577, Optical Modeling and Performance Predictions VII, 957703 (23 September 2015); doi: 10.1117/12.2188371; https://doi.org/10.1117/12.2188371
12. Brooks, Thomas E, "Predictive thermal control applied to HabEx", Proc. SPIE 10398, UV/Optical/IR Space Telescopes and Instruments: Innovative Technologies and Concepts VIII, 1039814 (5 Sept 2017); doi: 10.1117/12.2274338; https://doi.org/10.1117/12.2274338
13. Brooks, Thomas E., "Computed Tomography and Stiction in a Low Temperature Slumped Mirror," Mirror Technology Days in the Government (2017)
14. Eng, Ron, "Cryogenic optical and mechanical test result of a 1.5-meter lightweighted ULE mirror assembly" SPIE Proceedings 10742, August 2018
15. Brooks, Thomas E. and R. Eng, *"1.5-m ULE® Cryo & Mechanical Test Results,"* Mirror Technology Days in the Government (2017)
16. Brooks, Thomas E., Ron Eng, H. Phillip Stahl, "Optothermal stability of large ULE and Zerodur mirrors," Proc. SPIE 10743, Optical Modeling and Performance Predictions X, 107430A (17 September 2018)
17. Edwards, Mary J., "Today's ULE® Material of Choice for Premier Optics", Mirror Technology Days in the Government (2018)
18. Bijan Nemati, H. Philip Stahl, Mark T. Stahl, Garreth Ruane, "HabEx Telescope WFE stability specification derived from coronagraph starlight leakage," Proc. SPIE 10743, Optical Modeling and Performance Predictions X, 107430G (17 September 2018)
19. Brooks, Thomas E., Ron Eng, Tony Hull, H. Philip Stahl, "Modeling the Extremely Lightweight Zerodur Mirror (ELZM) thermal soak test", Proc. SPIE 10374, Optical Modeling and Performance Predictions IX, 103740E (6 September 2017); doi: 10.1117/12.2274084; http://dx.doi.org/10.1117/12.2274084
20. Stahl, H. Philip, "Overview and performance prediction of the baseline 4-meter telescope concept design for the habitable-zone exoplanet observatory", Proc. SPIE 10698, Space Telescopes and Instrumentation 2018, 106980W (6 July 2018); doi: 10.1117/12.2315291; https://doi.org/10.1117/12.2315291
21. Arnold, William R., H. Philip Stahl, "Design trade Study for a 4-meter off-axis primary mirror substrate and mount for the Habitable-zone Exoplanet Direct Imaging Mission", Proc. SPIE 10398, UV/Optical/IR Space Telescopes and Instruments: Innovative Technologies and Concepts VIII, 1039808 (5 September 2017); doi: 10.1117/12.2275193; http://dx.doi.org/10.1117/12.2275193